Nonequilibrium Transport at a Dissipative Quantum Phase Transition

Chung-Hou Chung,[1] Karyn Le Hur,[2] Matthias Vojta,[3] and Peter Wölfle[4,5]

[1]*Electrophysics Department, National Chiao-Tung University, HsinChu, Taiwan*
[2]*Department of Physics and Applied Physics, Yale University, New Haven, Connecticut, USA*
[3]*Institut für Theoretische Physik, Universität zu Köln, 50937 Köln, Germany*
[4]*Institut für Theorie der Kondensierten Materie, Universität Karlsruhe, 76128 Karlsruhe, Germany*
[5]*INT, Forschungszentrum Karlsruhe, 76021 Karlsruhe, Germany*

(Received 23 November 2008; published 28 May 2009)

We investigate the nonequilibrium transport near a quantum phase transition in a generic and relatively simple model, the dissipative resonant level model, that has many applications for nanosystems. We formulate a rigorous mapping and apply a controlled frequency-dependent renormalization group approach to compute the nonequilibrium current in the presence of a finite bias voltage V and a finite temperature T. For $V \to 0$, we find that the conductance has its well-known equilibrium form, while it displays a distinct nonequilibrium profile at finite voltage.

DOI: 10.1103/PhysRevLett.102.216803 PACS numbers: 73.23.−b, 03.65.Yz, 72.15.Qm

In recent years, quantum phase transitions (QPTs) [1,2] have attracted much attention at the nanoscale [3–8]. A finite bias voltage applied across a nanosystem is expected to smear out the equilibrium transition, but the current-induced decoherence might act quite differently as compared to thermal decoherence at finite temperature T, resulting in exotic behavior near the transition. Nonequilibrium effects at a quantum phase transition appear as an emerging field both in experimental and theoretical condensed matter physics [9–12]. Quantum impurity systems out of equilibrium are also extensively studied theoretically [13]. In this Letter, we aim to answer several fundamental questions related to the nonequilibrium transport in quantum dot settings, such as what is the scaling behavior of the conductance at zero temperature and finite bias voltage near the transition.

For this purpose, we employ a typical nanomodel comprising a dissipative resonant level (quantum dot). In this model, the QPT separating the conducting and insulating phase for the level is solely driven by dissipation, which can be modeled by a bosonic bath. Dissipation-driven QPTs have been addressed theoretically and experimentally in various systems, such as: Josephson junction arrays [14], superconducting thin films [15], superconducting qubits [16], and biological systems [17].

Our Hamiltonian takes the precise form:

$$H = \sum_{k,i=1,2} [\epsilon(k) - \mu_i] c_{ki}^\dagger c_{ki} + t_i c_{ki}^\dagger d + \text{H.c.} + \sum_r \lambda_r (d^\dagger d - 1/2)(b_r + b_r^\dagger) + \sum_r \omega_r b_r^\dagger b_r, \quad (1)$$

where t_i is the (real) hopping amplitude between the lead i and the quantum dot, c_{ki} and d are electron operators for the (Fermi-liquid type) leads and the quantum dot, respectively. $\mu_i = \pm V/2$ is the chemical potential applied on the lead i, while the dot level is at zero chemical potential.

To simplify the discussion, we assume that the electron spins have been polarized through the application of a strong magnetic field. Here, b_α are the boson operators of the dissipative bath, that is governed by an ohmic spectral density [4]: $J(\omega) = \sum_r \lambda_r^2 \delta(\omega - \omega_r) = \alpha\omega$. We use units in which $\hbar = 1$ and electric charge $e = 1$.

In equilibrium ($V = 0$), such a dissipative system comprising several leads maps onto the anisotropic one-channel Kondo model; we denote by t the hopping amplitude between the (effective) lead and the level. We introduce the dimensionless transverse Kondo coupling $g_\perp^{(e)}$ which is proportional to t (the exact prefactor is given in Refs. [4–6]) and the longitudinal coupling $g_z^{(e)} \propto 1 - \sqrt{\alpha}$ [4–6]. The model exhibits a Kosterlitz-Thouless (KT) QPT from a delocalized (Kondo screened) phase for $g_\perp^{(e)} + g_z^{(e)} > 0$, with a large conductance, $G \approx 1/h$ ($e = 1$ and $h = 2\pi\hbar = 2\pi$), to a localized (local moment) phase for $g_\perp^{(e)} + g_z^{(e)} \leq 0$, with a small conductance, as the dissipation strength is increased (see Fig. 1). For $g_\perp^{(e)} \to 0$, the KT

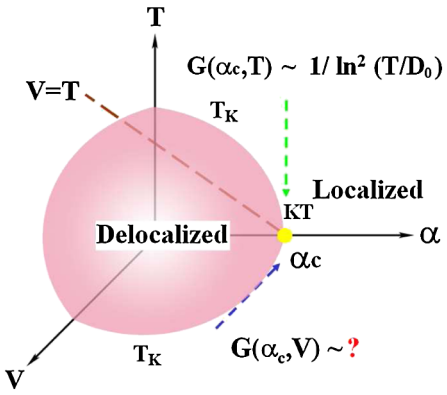

FIG. 1 (color online). Schematic phase diagram as a function of temperature T, dissipation strength α, and bias voltage V.

transition occurs at $\alpha_c = 1$. As $\alpha \to \alpha_c$, the Kondo temperature T_K obeys $\ln T_K \propto 1/(\alpha - \alpha_c)$ [3].

In equilibrium, the scaling functions $g_\perp^{(e)}(T)$ and $g_z^{(e)}(T)$ at the quantum critical point are obtained via the renormalization-group (RG) equations of the anisotropic Kondo model: $g_{\perp,\mathrm{cr}}^{(e)}(T) = -g_{z,\mathrm{cr}}^{(e)}(T) = [2\ln(T_D/T)]^{-1}$; hereafter, we introduce the energy scale $T_D = D_0 e^{1/(2g_\perp)}$, with D_0 being the ultraviolet cutoff and we set the Boltzmann constant $k_B = 1$. Having in mind a quantum dot at resonance, $D_0 = \min(\delta\epsilon, \omega_c)$, with $\delta\epsilon$ being the level spacing on the dot and ω_c the cutoff of the bosonic bath; D_0 is of the order of a few Kelvins. At the KT quantum phase transition, the conductance drops abruptly [7]:

$$G_{\mathrm{eq}}(\alpha_c, T \ll D_0) \propto [g_{\perp,\mathrm{cr}}^{(e)}(T)]^2 \propto \frac{1}{\ln^2(T/T_D)}. \quad (2)$$

Below, we analyze the nonequilibrium ($V \neq 0$) transport at the phase transition and in the localized phase.

First, we envision a nonequilibrium mapping revealing that the leads are controlled by distinct chemical potentials. Through similar bosonization and refermionization procedures as in equilibrium [3–6], our model is mapped onto an anisotropic Kondo model with the effective (Fermi-liquid) left (L) and right lead (R) [18]:

$$H_K = \sum_{k,\gamma=L,R,\sigma=\uparrow,\downarrow} [\epsilon_k - \mu_\gamma] c_{k\gamma\sigma}^\dagger c_{k\gamma\sigma} + (J_\perp^1 s_{LR}^+ S^- + J_\perp^2 s_{RL}^+ S^- + \mathrm{H.c.}) + \sum_{\gamma=L,R} J_z s_{\gamma\gamma}^z S^z, \quad (3)$$

where $c_{kL(R)\sigma}^\dagger$ is the electron operator of the effective lead $L(R)$, with σ the spin quantum number, $S^+ = d^\dagger$, $S^- = d$, and $S^z = Q - 1/2$ where $Q = d^\dagger d$ describes the charge occupancy of the level. Additionally, $s_{\gamma\beta}^{\pm} = \sum_{\alpha,\delta,k,k'} 1/2 c_{k'\gamma\alpha}^\dagger \sigma_{\alpha\delta}^{\pm} c_{k'\beta\delta}$ are the spin-flip operators between the effective leads γ and β, $J_\perp^{1(2)} \propto t_{1(2)}$ embody the transverse Kondo couplings, $J_z \propto 1/2(1 - 1/\sqrt{2\alpha^*})$, and $\mu_\gamma = \pm\frac{V}{2}\sqrt{1/(2\alpha^*)}$, where $1/\alpha^* = 1 + \alpha$. It should be noted that this mapping is exact near the phase transition where $\alpha \to 1$ or $\alpha^* \to 1/2$, and thus $\mu_\gamma = \pm V/2$.

From the mapping, $N_1 - N_2 = (N_L - N_R)$, where $N_i = \sum_{ki} c_{ki}^\dagger c_{ki}$ represents the charge in lead $i = 1, 2$, whereas $N_\gamma = \sum_k c_{k\gamma\sigma}^\dagger c_{k\gamma\sigma}$ represents the charge in the effective lead $\gamma = L, R$. This allows us to check that the averaged currents within the Keldysh formalism are the same in the original and in the effective Kondo model. Thus, the current I can be computed from the Kondo model.

The poor-man scaling equations of Anderson are generalized to nonequilibrium RG equations by including the frequency dependence of the Kondo couplings and the decoherence due to the steady-state current at finite bias voltage [19]. For the sake of clarity, we assume that the resonant level (quantum dot) is symmetrically coupled to the right and to the left lead, $t_1 = t_2$. The dimensionless Kondo couplings then have the extra symmetry (ω is the frequency): $g_{\perp(z)}(\omega) = g_{\perp(z)}(-\omega)$ where $g_{\perp(z)} = N(0)J_{\perp(z)}$ with $N(0)$ being the density of states per spin of the conduction electrons. We obtain [19]:

$$\frac{\partial g_z(\omega)}{\partial \ln D} = -\sum_{\beta=-1,1} \left[g_\perp\left(\frac{\beta V}{2}\right)\right]^2 \Theta_{\omega+\beta V/2}$$
$$\frac{\partial g_\perp(\omega)}{\partial \ln D} = -\sum_{\beta=-1,1} g_\perp\left(\frac{\beta V}{2}\right) g_z\left(\frac{\beta V}{2}\right) \Theta_{\omega+\beta V/2}, \quad (4)$$

where $\Theta_\omega = \Theta(D - |\omega + i\Gamma|)$, $D < D_0$ is the running cutoff, and Γ is the decoherence (dephasing) rate at finite bias which cuts off the RG flow [19]. The configurations of the system out of equilibrium are not true eigenstates, but acquire a finite lifetime. The spectral function of the fermion on the level is peaked at $\omega = \pm V/2$, and therefore we have $g_{\perp(z)}(\omega) \approx g_{\perp(z)}(\pm V/2)$ on the right hand side of Eq. (4). Other Kondo couplings are not generated.

In the Kondo model, Γ corresponds to the relaxation rate due to spin flip processes (which are charge flips in the original model). From Ref. [19], we identify:

$$\Gamma = \frac{\pi}{4} \sum_{\gamma,\gamma',\sigma} \int d\omega [n_\sigma g_z^2(\omega) f_{\omega-\mu_\gamma}(1 - f_{\omega-\mu_{\gamma'}}) + n_\sigma g_\perp^2(\omega) f_{\omega-\mu_\gamma}(1 - f_{\omega-\mu_{\gamma'}})], \quad (5)$$

where f_ω is the Fermi function. Here, $\gamma = \gamma'$ for the $g_z^2(\omega)$ terms while $\gamma \neq \gamma'$ for the $g_\perp^2(\omega)$ terms with γ, γ' being L or R. We have introduced the occupation numbers n_σ for up and down spins satisfying $n_\uparrow + n_\downarrow = 1$ and $S_z = 1/2(n_\uparrow - n_\downarrow)$. In the delocalized phase, we get $n_\uparrow = n_\downarrow = 1/2$ in agreement with the quantum Boltzmann equation [19]; at the phase transition we can use that $g_\perp(\omega) = -g_z(\omega)$ and that $\sum_\sigma n_\sigma = 1$, and finally in the localized phase $g_\perp \leq -g_z$, n_σ satisfies $|S_z| \to 1/2$ [3–6].

Following the scheme of Ref. [19], we solve Eqs. (4) and (5) self-consistently. First, we compute $g_{\perp(z)}(\omega = \pm V/2)$ for a given cutoff D. Second, we substitute the solutions back into the RG equations to get the general solutions for $g_{\perp(z)}(\omega)$ at finite V, and then extract the solutions in the limit $D \to 0$. When the cutoff D is lowered, the RG flows are not cut off by V but continue to flow for $\Gamma < D < V$ until they are stopped for $D < \Gamma$.

At the KT transition, we both numerically and analytically solve Eqs. (4) and (5) (in the limit of $D \to 0$):

$$g_{\perp,\mathrm{cr}}(\omega) = \sum_\beta \Theta(|\omega - \beta V/2| - V) \frac{1}{4\ln\left[\frac{T_D}{|\omega-\beta V/2|}\right]} + \Theta(V - |\omega - \beta V/2|) \times \left[\frac{1}{\ln[T_D^2/V \max(|\omega - \beta V/2|, \Gamma)]} - \frac{1}{4\ln\frac{T_D}{V}}\right]. \quad (6)$$

The solutions at the transition (denoted $g_{\perp,\mathrm{cr}}$ and $g_{z,\mathrm{cr}}$) are shown in Fig. 2. Since $g_{\perp,\mathrm{cr}}(\omega)$ decreases under the RG

scheme, the effect of the decoherence leads to the minima; the couplings are severely suppressed at the points $\omega = \pm\frac{V}{2}$. We also check that $g_{\perp,\mathrm{cr}}(\omega) = -g_{z,\mathrm{cr}}(\omega)$.

From the Keldysh calculation up to second order in the tunneling amplitudes, the current reads:

$$I = \frac{\pi}{8}\int d\omega\Big[\sum_{\sigma} 4g_{\perp}(\omega)^2 n_{\sigma} \times f_{\omega-\mu_L}(1-f_{\omega-\mu_R})\Big] - (L \leftrightarrow R). \tag{7}$$

At $T = 0$, it simplifies as $I = \frac{\pi}{2}\int_{-V/2}^{V/2} d\omega g_{\perp}^2(\omega)$. Then, we numerically evaluate the nonequilibrium current. The conductance is obtained from $G(V) = dI/dV$. The $T = 0$ results at the KT transition are shown in Fig. 3. First, it is instructive to compare the nonequilibrium current at the transition to the approximate expression:

$$I(\alpha_c, V) \approx \frac{\pi V}{2}\Big[\frac{\pi}{4}[g_{\perp,\mathrm{cr}}(\omega=0)]^2\Big] + \frac{\pi V}{2}\Big[\Big(1-\frac{\pi}{4}\Big)[g_{\perp,\mathrm{cr}}(\omega=V/2)]^2\Big], \tag{8}$$

where $g_{\perp,\mathrm{cr}}(\omega=0) \approx 2\big(\frac{1}{\ln(2T_D^2/V^2)} - \frac{1}{4\ln(T_D/V)}\big)$, and $g_{\perp,\mathrm{cr}}(\omega=V/2) \approx 1/\ln(\frac{T_D^2}{\Gamma V})$. We have treated $g_{\perp,\mathrm{cr}}(\omega)^2$ within the interval $-V/2 < \omega < V/2$ as a semi-ellipse.

As demonstrated in Fig. 3, the conductance $G(V)$ obtained via the approximation in Eq. (8) fits very well with that obtained numerically over a whole range of $0 < V < D_0$. In the low-bias $V \to 0$ (equilibrium) limit, since $g_{\perp,\mathrm{cr}}(\omega=0) \approx g^{(e)}_{\perp,\mathrm{cr}}(T=V) \ll 1$, we have $I(\alpha_c, V) \approx \frac{\pi V}{2}[g^{(e)}_{\perp,\mathrm{cr}}(T=V)]^2$; therefore the scaling of $G(\alpha_c, V)$ is reminiscent of the equilibrium expression in Eq. (2), $G(\alpha_c, V) \approx \frac{\pi}{2}[g^{(e)}_{\perp,\mathrm{cr}}(T=V)]^2 = \frac{\pi}{8}\frac{1}{\ln^2(T_D/V)}$. This agreement between equilibrium and nonequilibrium conductance at low V persists up to a crossover scale $V \approx 0.01D_0$ (determined for the parameters used in Fig. 3). At larger biases, the conductance shows a unique nonequilibrium profile; see Eq. (8). We find an excellent agreement of the nonequilibrium conductance obtained by three different ways—pure numerics, analytical solution Eq. (6), and the approximation in Eq. (8).

The distinct nonequilibrium scaling behavior seen here is in fact closely tied to the nontrivial (nonlinear) V dependence of the decoherence rate $\Gamma(V)$. In particular, at the KT transition, we find that $\Gamma \sim \frac{1}{2}I$ is a highly nonlinear function in V, resulting in the deviation of the nonequilibrium scaling from that in equilibrium. For large bias voltages $V \to D_0$, since $g_{\perp,\mathrm{cr}}(\omega)$ approaches its bare value $g_{\perp}$, the nonequilibrium conductance increases rapidly and reaches $G(\alpha_c, V) \approx G_0 = \frac{\pi}{2}g_{\perp}^2$. The nonequilibrium conductance is smaller than the equilibrium one, $G(\alpha_c, V) < G_{\mathrm{eq}}(\alpha_c, T=V)$, since $g_{\perp}(\omega = \pm V/2) < g_{\perp}(\omega=0)$. Additionally, in the delocalized phase for $V \gg T_K > 0$, the RG flow of $g_{\perp}$ is suppressed by the decoherence rate, and $G \propto 1/\ln^2(V/T_K)$ [19].

In the localized phase, the equilibrium RG equations of the effective Kondo model can be solved analytically, resulting in $G^{(e)}_{\mathrm{loc}}(T) = \frac{\pi}{2}[g^{(e)}_{\perp,\mathrm{loc}}(T)]^2$, where

$$g^{(e)}_{\perp,\mathrm{loc}}(T) = \frac{2cg_{\perp}(c+|g_z|)}{(c+|g_z|)^2 - g_{\perp}^2(\frac{T}{D_0})^{4c}}\Big(\frac{T}{D_0}\Big)^{2c}, \tag{9}$$

with $c = \sqrt{g_z^2 - g_{\perp}^2}$. We introduce the energy scale $T^* = D_0 e^{-\pi/\sqrt{g_z^2-g_{\perp}^2}}$ (which vanishes at the KT transition) such that $g^{(e)}_{\perp,\mathrm{loc}}(T) \propto (T/T^*)^{2c}$ for $T \to 0$, leading to $G^{(e)}_{\mathrm{loc}}(T) \propto (T/T^*)^{4c}$.

For very small bias voltages $V \to 0$, we find that the conductance reduces to the equilibrium scaling: $G(V) \to G^{(e)}_{\mathrm{loc}}(T=V) \propto (V/T^*)^{4c}$ [see Figs. 4(a) and 4(b)]. For $g_{\perp,\mathrm{loc}} \ll |g_{z,\mathrm{loc}}|$ and $\alpha^* \to 1/2$, we get that the exponent $4c \approx 2\alpha^* - 1$, in perfect agreement with that obtained in equilibrium at low temperatures: $G(T) \propto T^{2\alpha^*-1}$ [7]. At higher bias voltages $0.01D_0 < V < D_0$, the conductance now follows a unique nonequilibrium form [consult Fig. 4(c)].

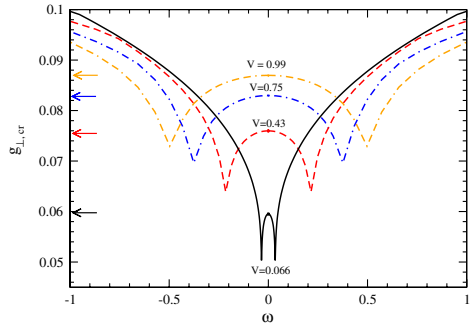

FIG. 2 (color online). $g_{\perp,\mathrm{cr}}(\omega) = -g_{z,\mathrm{cr}}(\omega)$ at $\alpha = \alpha_c$; the bare couplings are $g_{\perp} = -g_z = 0.1$. We have set $V = 0.066D_0$, $0.43D_0$, $0.75D_0$ and $0.99D_0$ where $D_0 = 1$ for all the figures. The arrows give the values of $g_{\perp,\mathrm{cr}}(\omega=0)$ at these bias voltages.

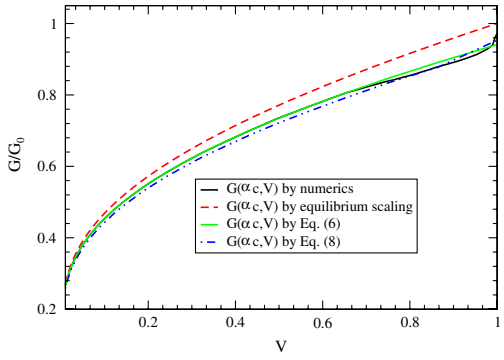

FIG. 3 (color online). Nonequilibrium conductance at the KT transition. G_0 is the equilibrium conductance at the transition for $T = D_0$: $G_0 = G_{\mathrm{eq}}(\alpha_c, T = D_0) = 0.005\pi$ with the bare couplings $g_{\perp} = -g_z = 0.1$. Again, we set the charge $e = \hbar = 1$.

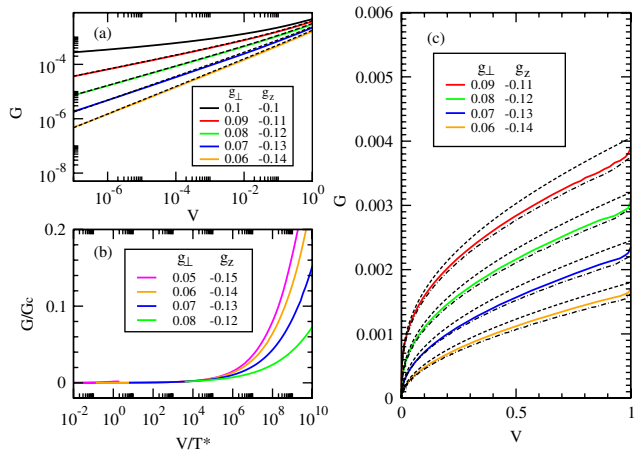

FIG. 4 (color online). Conductance in the localized phase (in units of $\pi/\hbar$). (a) $G(V)$ at low bias follows the equilibrium scaling (dashed lines). (b) The conductance $G(V)/G_c$ is a function of V/T^* where we have defined $G_c = G(\alpha_c, V)$ and $T^* = D_0 e^{-\pi/\sqrt{g_z^2 - g_\perp^2}}$. (c) At large bias voltages V, the nonequilibrium conductance $G(V)$ (solid lines) is distinct from the equilibrium form (dashed lines). The dot-dashed lines stem from an analytical approximation via Eq. (8).

We have also analyzed the finite temperature profile of the nonequilibrium conductance at the transition. We distinguish two different behaviors. For $V > T$, the conductance $G(V, T)$ follows the nonequilibrium form at $T = 0$ [see Fig. 5(a)], while for $V < T$ it follows the $(V = 0)$ finite-temperature expression [see Fig. 5(b)]. These two scaling behaviors have a crossover at $V = T$.

In summary, we have investigated the nonequilibrium transport at a QPT using a standard nanomodel, the dissipative resonant level. We have used an exact mapping and applied a controlled frequency-dependent renormalization group approach to compute the current. For $V \to 0$, the conductance G follows the equilibrium behavior; by increasing V, the frequency dependence of the couplings begins to play an important role and therefore we systematically find very distinct scalings. We have also analyzed the finite temperature profile of $G(V, T)$ at the transition and identified two distinct behaviors at $V > T$ and $V < T$. Finally, our results have a direct experimental relevance for dissipative two-level systems.

We are grateful to D. Goldhaber-Gordon and G. Zarand for stimulating discussions, and to R. T. Chang and K. V. P. Lata for technical support. We also acknowledge the generous support from the NSC Grant No. 95-2112-M-009-049-MY3, the MOE-ATU program, the NCTS of Taiwan, R.O.C. (C. H. C.), the Department of Energy in the USA under the Contract No. DE-FG02-08ER46541 (K. L. H.), the DFG via SFB 608 and SFB/TR-12 (M. V.), and the DFG-Center for Functional Nanostructures, C.F.N. (P. W.). C. H. C. has also benefitted from the visiting programs of KITP, ICTP, and MPI-PKS.

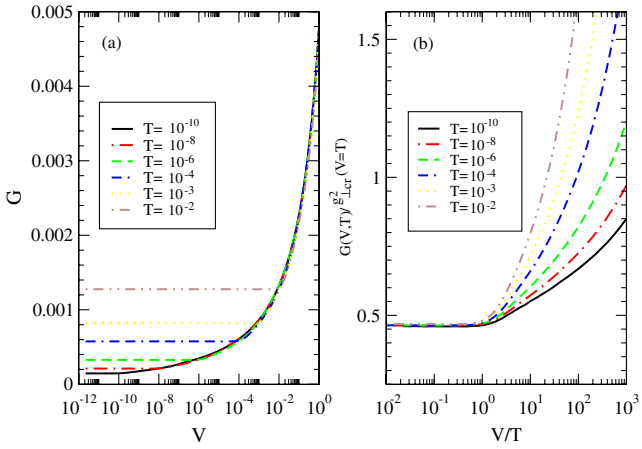

FIG. 5 (color online). Scaling of the conductance at the KT transition (same unit as in Fig. 3). (a) For $V > T$, the conductance follows the nonequilibrium scaling $G(\alpha_c, V)$. (b) For $V < T$, now the conductance follows the equilibrium scaling $G(\alpha_c, T)$.

[1] S. Sachdev, *Quantum Phase Transitions* (Cambridge University Press, Cambridge, England, 1999).
[2] S. L. Sondhi, S. M. Girvin, J. P. Carini, and D. Shahar, Rev. Mod. Phys. **69**, 315 (1997).
[3] K. Le Hur, Phys. Rev. Lett. **92**, 196804 (2004); M.-R. Li, K. Le Hur, and W. Hofstetter, Phys. Rev. Lett. **95**, 086406 (2005).
[4] K. Le Hur and M.-R. Li, Phys. Rev. B **72**, 073305 (2005).
[5] P. Cedraschi and M. Büttiker, Ann. Phys. (N.Y.) **289**, 1 (2001).
[6] A. Furusaki and K. A. Matveev, Phys. Rev. Lett. **88**, 226404 (2002).
[7] L. Borda *et al.*, arXiv:cond-mat/0602019.
[8] G. Zarand *et al.*, Phys. Rev. Lett. **97**, 166802 (2006).
[9] D. E. Feldman, Phys. Rev. Lett. **95**, 177201 (2005).
[10] A. Mitra *et al.*, Phys. Rev. Lett. **97**, 236808 (2006).
[11] R. M. Potok *et al.*, Nature (London) **446**, 167 (2007).
[12] S. Kirchner and Q. Si, arXiv:0805.3717.
[13] See, e.g., P. Mehta and N. Andrei, Phys. Rev. Lett. **96**, 216802 (2006); S. Kehrein, Phys. Rev. Lett. **95**, 056602 (2005); E. Boulat, H. Saleur, and P. Schmitteckert, Phys. Rev. Lett. **101**, 140601 (2008); B. Doyon, Phys. Rev. Lett. **99**, 076806 (2007).
[14] G. Refael, E. Demler, Y. Oreg, and D. S. Fisher, Phys. Rev. B **75**, 014522 (2007).
[15] N. Mason and A. Kapitulnik, Phys. Rev. B **65**, 220505(R) (2002).
[16] A. J. Rimberg *et al.*, Phys. Rev. Lett. **78**, 2632 (1997).
[17] J. Gilmore and R. McKenzie, J. Phys. C **11**, 2965 (1999).
[18] In the delocalized phase, it would be more judicious to redefine $\Psi \to (t_1 c_1 + t_2 c_2)/\sqrt{t_1^2 + t_2^2}$, and then bosonize and refermionize to get the fermions with spins [4], Ψ_σ.
[19] A. Rosch *et al.*, Phys. Rev. Lett. **90**, 076804 (2003); J. Phys. Soc. Jpn. **74**, 118 (2005).